Arab Gulf J. Scient. Res., 7 (2), pp. 39-54 (1989)

Surface Residual Stresses in Wet Underwater Steel Welds

Salman Dawod Mehdi, Sultan Abdul-Rassak Sultan, Abdul Karim Flaih Hassan

Department of Mechanical Engineering, College of Engineering, University of Basrah, Basrah, Iraq

ABSTRACT. The present work was to determine the residual stresses developed on the surface of welded plate in saline water using X-ray diffraction method.

Weld beads were deposited on carbon manganese steel under a 200 mm depth of both fresh and saline water using coated rutile electrodes type E 7012. Open air welds were also deposited for the purpose of comparison.

The residual stress levels were measured and compared for welds made under fresh and saline water with those obtained for normal open air welds made under the same set of welding parameters.

It was found that the maximum sum of the surface stresses in fresh and saline water welds were about 81% and 77% of the maximum sum of surface stresses that developed in the open air welds, respectively.

One of the undesirable results of welding is the development of residual stresses in the welds and welded structure. The reasons for the development of these stresses are the localized heating and shrinkage of resolidified metal (Parmar 1978). In weldments made in low carbon steel, the maximum residual stresses is frequently as high as the yield stress of the weld metal (Masubuchi 1980).

Residual stresses are developed in all directions in butt welded plate (Noyan *et al.* 1985, Ruud *et al.* 1985) but the important stresses are those parallel to the weld designated σ_x, and those transverse to it designated σ_y. (Fig. 1b) shows the theoretical of the longitudinal residual stress σ_x. Tensile stresses of high magnitude are produced in the region near the weld; these taper off rapidly and become compressive after a distance several time the width of the weld metal. According to Masbuchi and Martine analysis (Masubchi 1980) the distribution of the longitudinal residual stress σ_x (Fig. 1b) can be approximated by the following equation:

$$\sigma_x (y) = \sigma_m \left[1 - \left(\frac{y}{b}\right)^2\right] e^{-\frac{1}{2}(y/b)^2} \quad (1)$$

The distribution of the transverse residual stress, σ_y, along the length of the weld is shown in (Fig. 1c). Tensile stresses of relatively low magnitude are produced in the middle-part of the joint and compressive stresses at the ends of it.

Parmar (1978) was one of the researchers who have drawn an attention to study residual stresses in underwater welds. He found out that the maximum sum of residual stresses which developed in underwater welds was about 75% of that developed in open air welds.

This study concentrates on the surface residual stresses that developed in welded steel plate and presents a comparison of the magnitude of these stresses in both fresh and saline water as well as in open air welds.

Stress Analysis

X-ray diffraction has been used to determine residual stresses by measuring interplaner spacings (d-values) in weldments containing residual stresses and in stress relieved control samples. The relation between the residual stresses and the interplaner spacing (d-values) can be expressed as follows (Barrett and Massalski 1980, and Singh 1982):

$$\sigma_1 + \sigma_2 = -\frac{E}{\nu} \times \frac{\triangle d}{d}$$

$$= -\frac{E}{\nu}\left(\frac{ds-du}{du}\right) \quad (2)$$

Experimental Procedure

Weld beads were deposited on a carbon manganise steel plate of 8mm thickness. The chemical analyses of the steel plate is given in Table 1. The mechanical properties of this type of steel is illustrated in Table 2. Semi-mechanized welding process was carried out with coated rutile electrodes of 4mm core wire diameter in a downhand position as shown in (Fig. 2). The welding parameters are given in Table 3.

Square specimens of 26 × 26 mm were cut from both underwater and open air welded plate as well as from the original base plate. The weld beads of

Table 1. Chemical composition of the steel plate and electrode wire used

Element	% in steel plate	% in electrode
C	0.13	0.16
Cr	0.20	0.13
Mn	0.70	0.56
Si	0.074	0.15

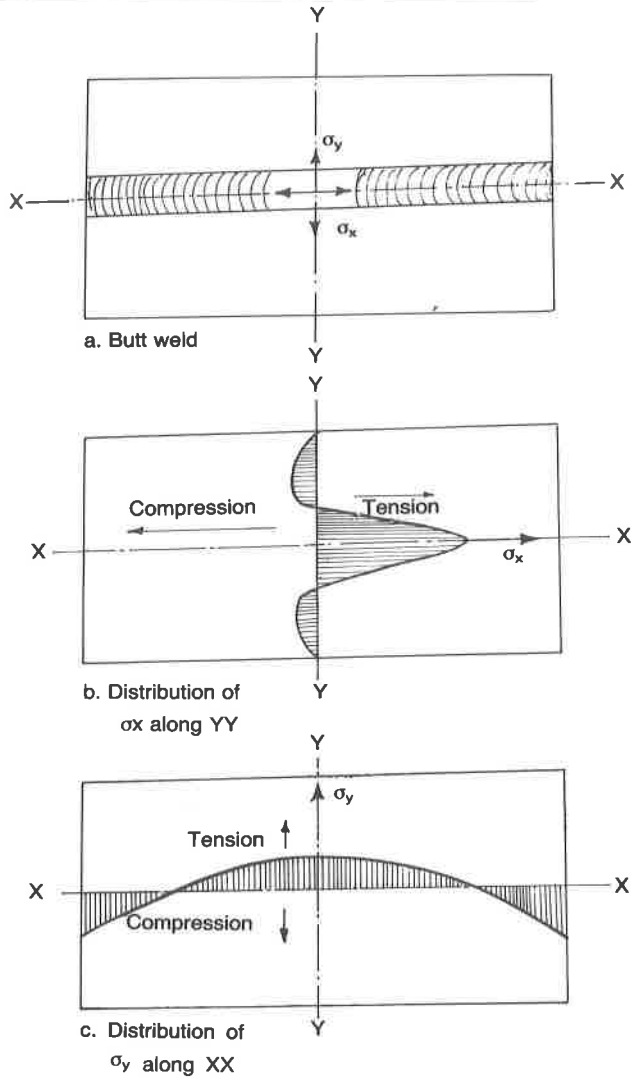

Fig. 1. Typical distribution of residual streses in a butt weld (Masubuchi 1980)

Table 2. Mechanical properties of the steel plate used

Ultimate tensile strength	366.24 N/mm^2
Yield point	294.30 N/mm^2
Percent of elongation	23%
Percent of reduction in area	63%
Young modulus	2.015×10^5 N/mm^2
Poisson's ratio	0.28

Table 3. Parameters of welding process

Power source	AC
Welding current	200 Amp.
Arc voltage	22 volts
Welding speed	6 mm/sec.
Electrode feed rate	14 mm/sec.
Height of water column for underwater welding	200 mm
Heat input equation	$= \zeta a \frac{IV}{v}$

approximatly 10 mm width of the prepared specimens were kept, as far as possible, in the center. The original base plate specimen was annealed at 450°C and cooled slowly. The reverse sides of the welded specimens and one side of the annealed specimen were polished and lightly etched. The etched sides of the welded specimen were marked with a line perpendicular to the weld direction in the midpoint of it. A similar line was also marked on the annealed specimen. These lines were further divided into ten parts as shown in (Fig. 3).

The specimens were tested by placing them in the diffractometre. As Mo kα radiation was used, the best set of (hk1) crystallographic planes for back reflection was (220) (Ruud *et al.* 1985 and Singh 1982) which carefully scanned. The proper setting of the counter to the diffracted beam to give best result was at 40.50°. For every point used on the specimens, different angles covering a range of (38° to 42°) were studied in order to get the value of (2θ) for Mo kα peak. The angular positions were scanned for each of these points on the specimens at an interval of (0.01°) and with ratio (θ:2θ) for the specimen holder and counter, respectively. The reading of the counter for each time was recorded for 100 seconds. The recorded counter readings were plotted against (2θ) and fitted in its upper region with a parabola (Barrett and Massalski 1980) to find the exact (2θ) for kα peak for each point scanned. This is usually done by using three point data of the recorded peak as is shown in (Fig. 4) and illustrated by the following relation (Barrett and Massalski 1980):

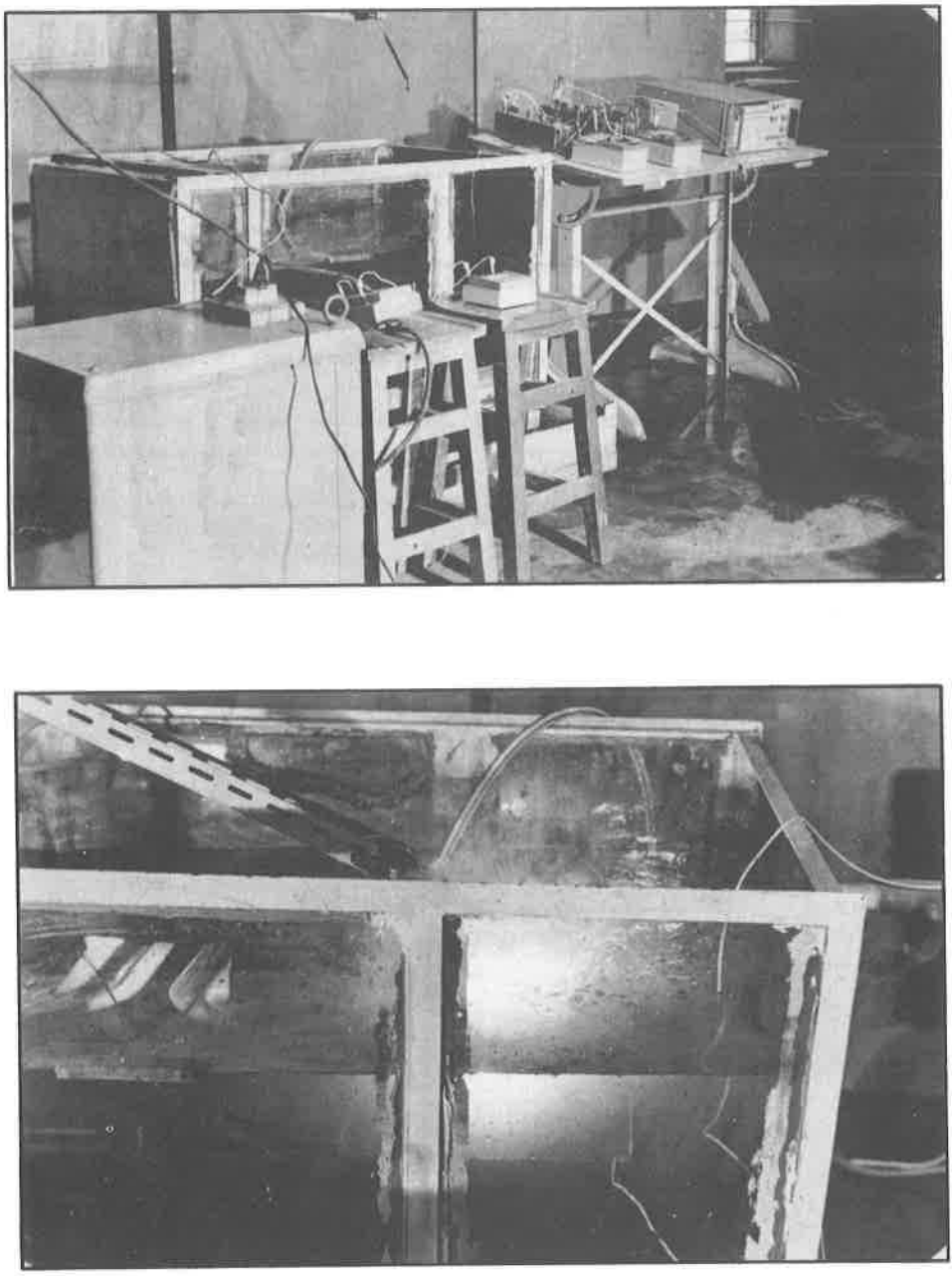

Fig. 2. Photographs of the underwater welding equipment

$$h = x_1 - \frac{c}{2}\left(\frac{3a+b}{a+b}\right) \quad (3)$$

The annealed specimen was, firstly used to determine the value of (du) which is the same at any point. The values (ds) were calculated for every point scanned using the following Bragg's equation (Verhovene 1975):

$$d = n\lambda / 2\sin\theta \quad (4)$$

The details of the exact values of (2θ) and (ds) for every point on the line in the welded specimens are given in Table 4. Knowing (du) and ds-value for each point, then, the sum of the surface stresses can be determined using equation 2. The magnitude of the surface stresses are given in Table 5.

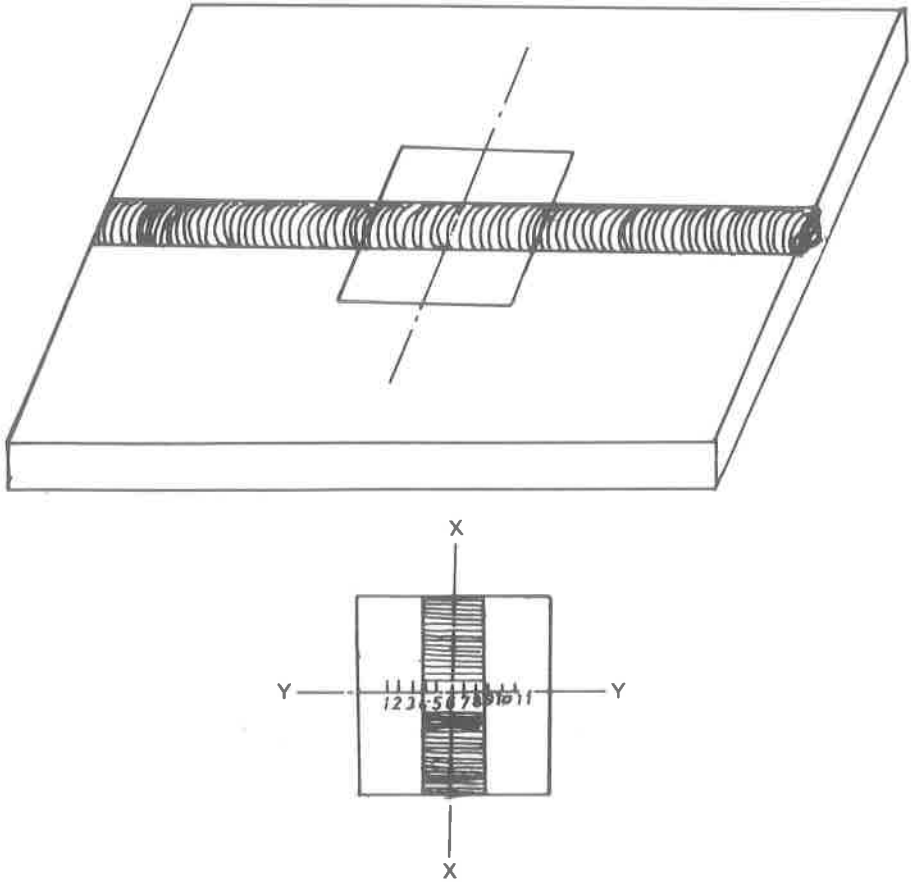

Fig. 3. The divisions of the marked line of the polished sides of welded specimens

Table 4. Details of exact (2θ) and ds-value of different welds

Distance from one edge (mm)	Air Weld		Fresh Water Weld		Saline Water Weld	
	2θ* at the peak (I)	ds × 10^{-7} (mm)	2θ* at the peak (I)	ds × 10^{-7} (mm)	2θ* at the peak (I)	ds × 10^{-7} (mm)
2	40° 29′ 53″	1.024699	40° 29′ 56″	1.024682	40° 29′ 57″	1.024679
4	40° 29′ 56″	1.024682	40° 29′ 53″	1.024703	40° 29′ 52″	1.024699
6	40° 30′ 04″	1.024629	40° 29′ 59″	1.024661	40° 29′ 56″	1.024685
8	40° 30′ 27″	1.024473	40° 30′ 18″	1.024332	40° 30′ 17″	1.024531
10	40° 30′ 49″	1.024332	40° 30′ 45″	1.024355	40° 30′ 41″	1.024382
12	40° 31′ 08″	1.024193	40° 30′ 44″	1.024361	40° 30′ 42″	1.024373
14	40° 30′ 48″	1.024331	40° 30′ 37″	1.024403	40° 30′ 36″	1.024413
16	40° 30′ 30″	1.024451	40° 30′ 35″	1.024417	40° 30′ 24″	1.024493
18	40° 30′ 05″	1.024621	40° 30′ 01″	1.024646	40° 30′ 02″	1.024645
20	40° 30′ 08″	1.024602	40° 29′ 51″	1.024712	40° 30′ 09″	1.024593
22	40° 30′ 09″	1.024594	40° 29′ 52″	1.024704	40° 30′ 07″	1.024609

* Angles are rounded off to the nearest second.

Table 5. Differences in interplaner-spacings and sum of surface stresses of different welds

Distance from one edge of a specimen (mm)	Open Air Welds			Under Fresh Water Welds			Under Saline Water Welds		
	$(ds-du)\times10^{-10}$ (mm)	$\frac{(ds-du)}{du}\times10^{-5}$	$\sigma_x+\sigma_y$ (N/mm^2)	$(ds-du)\times10^{-10}$ (mm)	$\frac{(ds-du)}{du}\times10^{-5}$	$\sigma_x+\sigma_y$ (N/mm^2)	$(ds-du)\times10^{-10}$ (mm)	$\frac{(ds-du)}{du}\times10^{-5}$	$\sigma_x+\sigma_y$ (N/mm^2)
2	+0.0458	+04.4783	−32.23	+0.0286	+02.7998	−20.15	+0.0259	+02.5372	−18.26
4	+0.0286	+02.7998	−20.15	+0.0501	+04.8979	−35.25	+0.0466	+04.5533	−32.77
6	−0.0237	−02.3135	+16.65	+0.0081	+00.7989	+05.75	+0.0319	+03.1208	−22.46
8	−0.1807	−17.5841	+126.55	−0.1211	−11.8274	+85.12	−0.1117	−10.9103	+78.52
10	−0.3306	−32.2711	+232.25	−0.2782	−27.1536	+195.42	−0.2708	−28.4366	+190.26
12	−0.3599	−35.1321	+252.84	−0.2922	−28.5194	+205.25	−0.2793	−27.2675	+196.24
14	−0.3213	−31.3637	+225.72	−0.2496	−24.3648	+175.35	−0.2396	−23.3922	+168.35
16	−0.2018	−19.6975	+141.76	−0.1357	−13.2447	+95.32	−0.1598	−15.5999	+112.27
18	−0.0319	−03.1194	+22.45	−0.0063	−00.6475	+04.66	+0.0082	+00.8031	−05.78
20	+0.0509	+04.9771	−35.82	+0.0594	+05.8025	−41.76	+0.0601	+05.8692	−42.24
22	+0.0686	+06.7001	−48.22	+0.0510	+04.9813	−35.85	+0.0437	+04.2741	−30.76

$du = 10.2465\times10^{-8}$mm, $E = 2.0151\times10^{5}$ N/mm^2, $\nu = 0.28$, $-E/\nu = -7.1967\times10^{5}$ N/mm^2

Results and Discussion

Table 5 shows the differences in the interplaner spacings of the stresed (welded) and the unstressed specimens [the (ds-du) values] along with the calculated values of the stresses for fresh and saline water welds and for open air

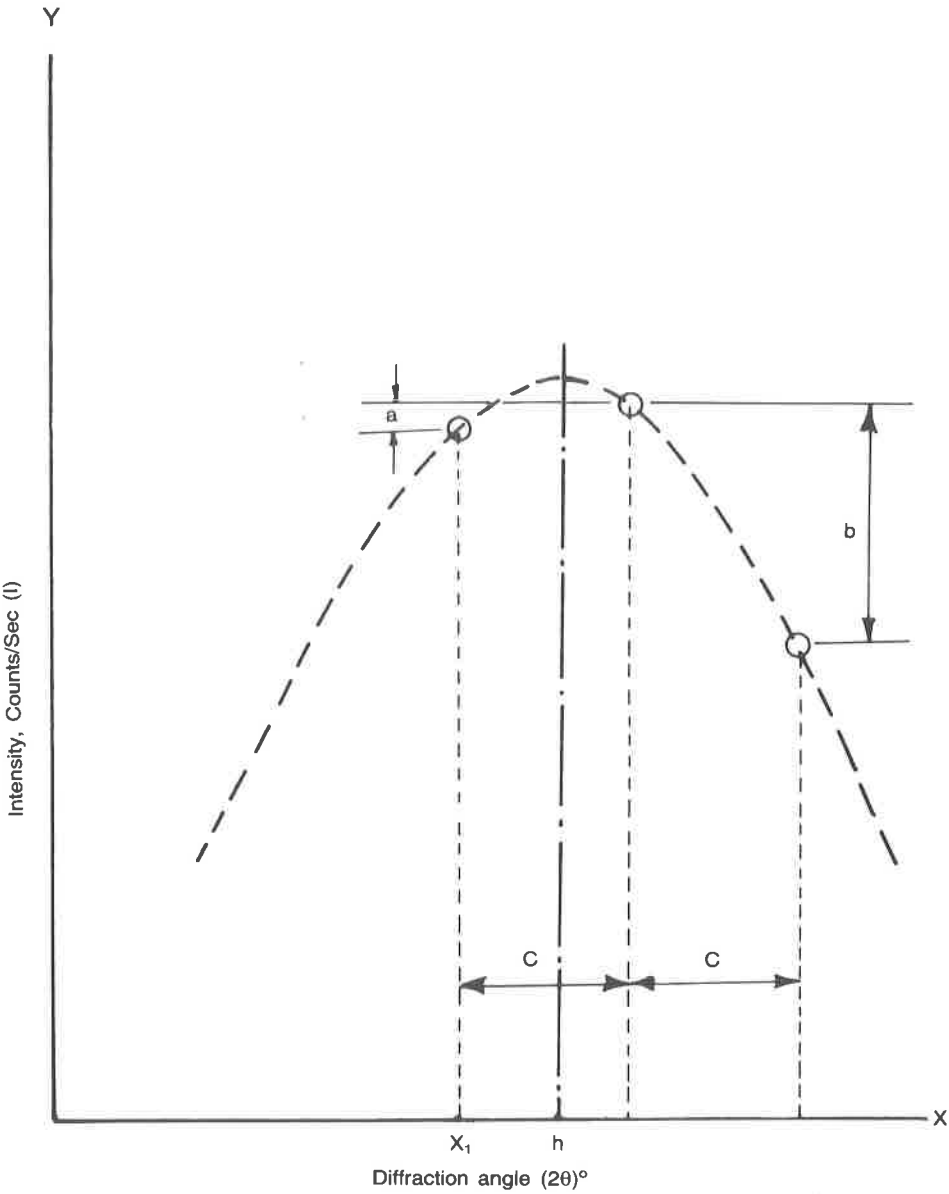

Fig. 4. Parabola fitting at three points data to a diffraction peak (Barrett *et al.* 1980)

welds. These values of the combined stresses were plotted against the distance (y-y) axis as shown in (Fig. 5). These stresses distributed along yy-axis include both longitudinal and transverse stresses which are disgnated as σ_x and σ_y, respectively. The sum of these stresses is as high as the value of the yield point of the weld zone in carbon manganized steel (Masubuchi 1980). Fig. 5 shows that the sum of these stresses is a little lower than the value of yield point of the metal that used. A similar result was also obtained by Parmar (1978). This is attributed to the stress level which introduced due to the cutting and grinding through specimen preparation. Cutting the specimen into a smaller size, as in the present study leaves it with a low value of transverse stress σ_y (Parmar 1978). The grinding process used on the surface of specimen can also leave it with some compressive stress which decreases in the magnitude as the distance increases a way from the surface (Masubuchi 1980). Rubbing the surface with paper that contain abrasive particles creates a compressive stress on the surface to the extent of about 60 N/mm^2 (Barret and Massalski 1980). Thus, the values of stresses that given in (Fig. 5) is the resultant of all the above factors and appears-in magnitude to be longitudenal stress σ_x.

On a comparison of patterns of the stresses for the three types of welds, it was found that the maximum of the sum of the stresses ($\sigma_x+\sigma_y$) developed in fresh water welds is 18.7% lower than that of the open air weld and those in saline water is 22.3% lower than that of the open air welds. Furthermore, the stresses developed in the saline water weld is 5% lower than those of fresh water welds. It was also noticed that the stress in the fresh water weld and in the saline water weld were confined to a smaller zone, compared with open the air, to the extent of 22.7% and 26.5%, respectively. The results of the present work agree with that found by Parmar (1978). Fig. 6 shows an abvious difference between the width underfresh and undersaline water weld zones. It is clear that the heat affected zone (HAZ) is narrower in saline water weld than in fresh water weld as it was illustrated in (Fig. 6). It was also found that (HAZ) is narrower in fresh water than in an open air weld. Same observation was found by Brown and Masubuchi (1975) and by Khan and Lai (1978). All above changes in the width of the weld metal and heat affected zones can be attributed to the effect of cooling rate during welding process. Cooling rate is higher in saline wter than in fresh water and it is lower in open air than in fresh water. In saline water, the presence of the salt causes a series of small explosions (Reed-Hill 1974) to occur near the hot surface and therefore violentily agitates the cooling medium in the vicinity of the weld plate and increases cooling rate. This means the heat sink is higher in saline water than in fresh water and than in the air. Therefore, the heat accumulated due to the heat source during welding operation on the welded plate is lower in case of saline water compared to that of the fresh water and the air. This gives lower distortion and results in lower residual stresses in saline water weld compared to fresh water and open air welds.

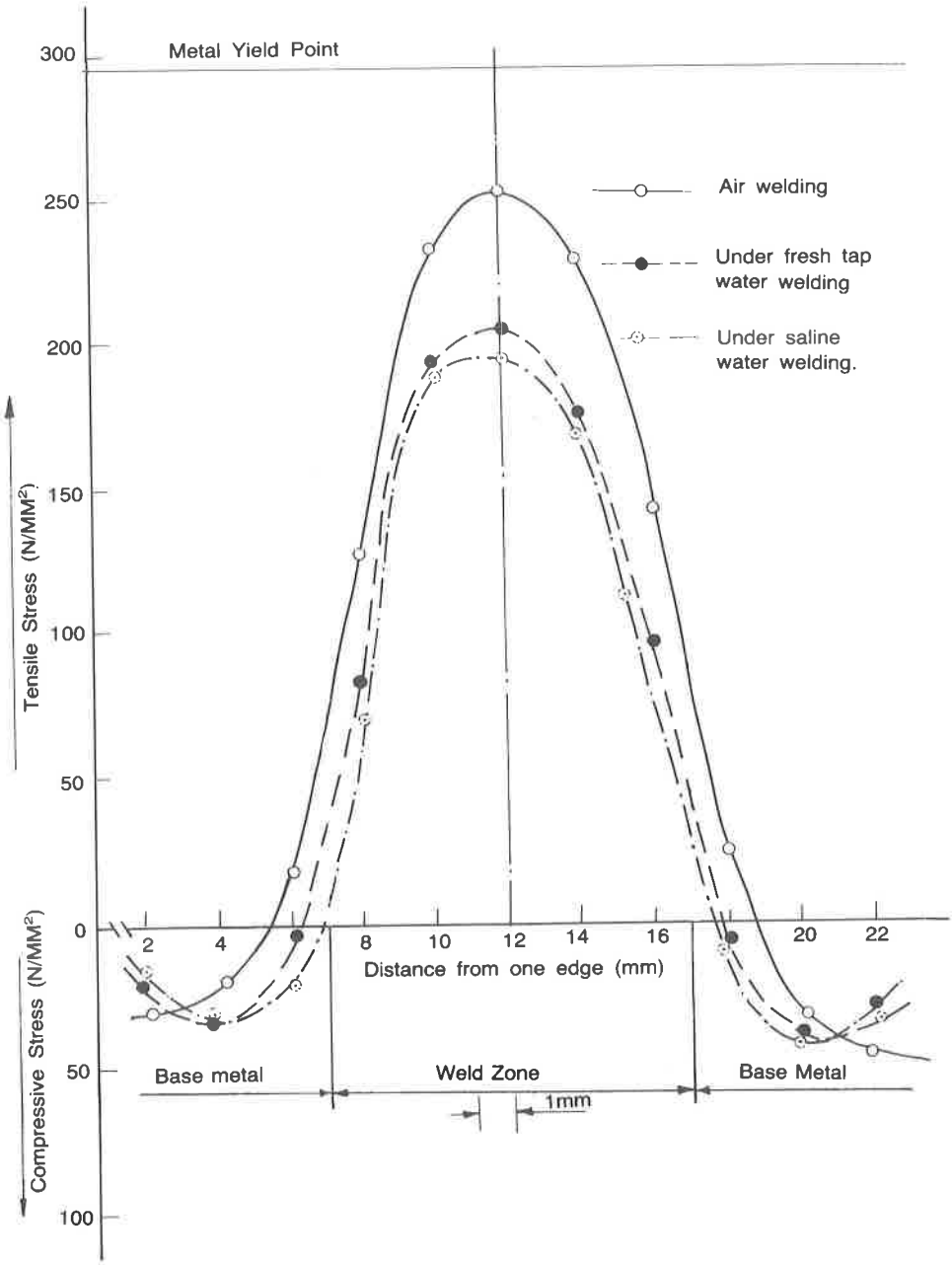

Fig. 5. Stress patterns of welding under different circumstances

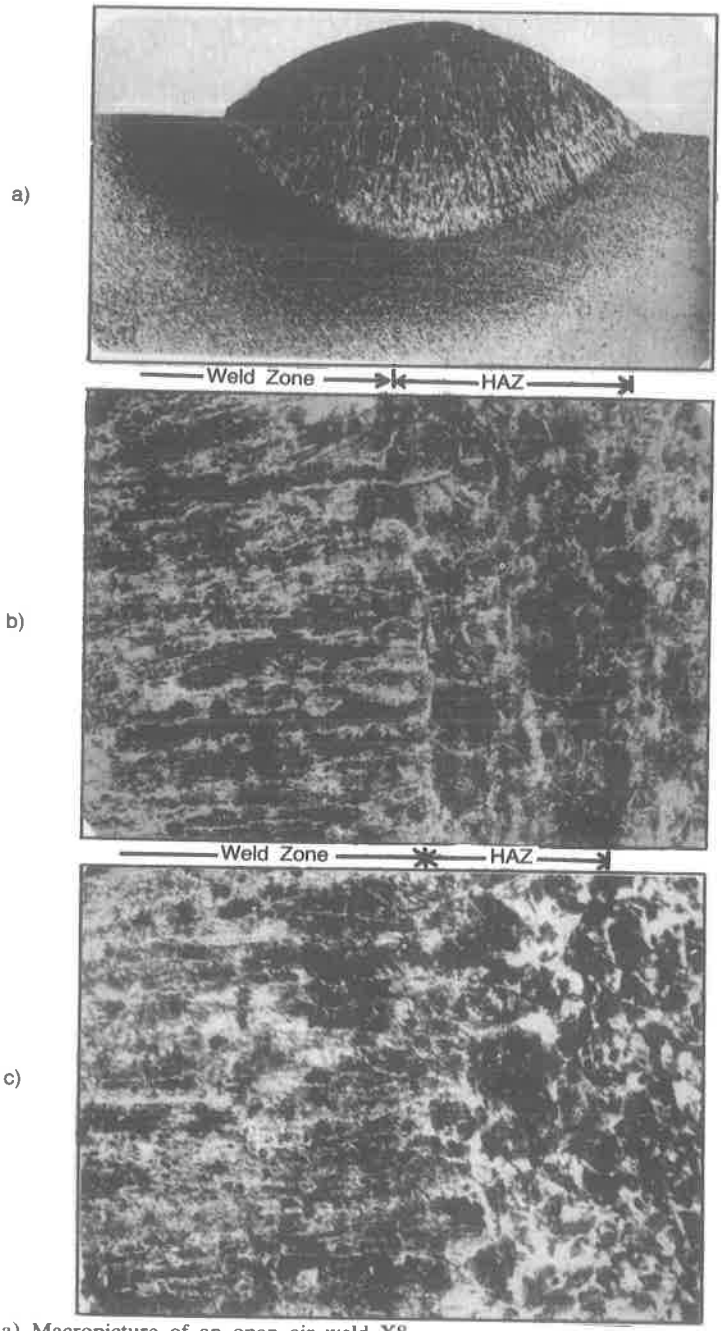

Fig. 6. a) Macropicture of an open air weld X8
b) Macropicture of under fresh water weld X120
c) Macropicture of under saline water weld X120

Conclusions

The surface residual stresses of the carbon manganise steel weld metal were examined with following conclusions:

(1) The maximum sum of the surface stresses developed in weld metal made under fresh water and under saline water are about 81% and 77% of those values developed in the open air weld, respectively.

(2) The maximum stresses developed in under fresh and under saline water welds, are confined to a narrower zone by the extent of 22.7% and 26.5% compared to that of an open air welds made under same set of welding parameters, respectively.

(3) The maximum stresses developed in a weld made under saline water is 5% lower than that of weld made under fresh water.

Nomenclature

σ_x (y)	= Longitudinal residual stress
σ_y (x)	= Transverse residual stress
$\sigma_1 + \sigma_2$	= The principle stresses
σm	= Maximum residual stress at weld region
b	= The width of the tension zone of the residual stress
y	= The transverse distance from the center of the weld
ds	= d-value for stressed sample
du	= d-value for unstressed sample
E	= Young's Modulus of the material
ν	= Poisson's ratio
h	= x-coordinate of the vertex
x_1	= Position of first data point
c	= Interval in the x-direction between data point
a,b	= Differences in the vertical coordinate (y) between the middle data point and data point on either side of it
θ	= Diffraction angle
d	= Interplaner spacing (d-value)
n	= Mode number (integer 1,2,....)
λ	= Wave length of X-rays (Å)
I	= Current (Amps)
V	= Voltage (volts)
v	= Welding speed (mm/sec.)
ζa	= Arc efficiency (0.75-0.85 for coated electrode)

References

Barrett, C.S., Massalski, T.B. (1980) Structure of Metals, Pergamon Press, London.

Brown, R.T., Masubuchi, K. (1975) Fundamental research on underwater welding; effect of water environment on metallurgical structure of weld, *Welding Journal,* **6:** 1785-1885.

Khan, M.I., Lai, S. (1978) Investigation of the effect of welding condition on the metallurgical transformation and mechanical properties of underwater welds, Afro-Asian Conference on Welding and Metal Technolog, Delhi, India, 1-8.

Masubuchi, K. (1980) Analysis of Welded Structures, Pergamon Press, Oxford 189-193.

Noyan, I.C., Cohen, J.B. (1985) An X-ray differaction study of the residual stress-strain distribution in shot peened two-phase brass, *Material Science and Engineering,* **75:** 179-193.

Parmar, R.S. (1978) Residual stresses in underwater weld, IE(I) *Journal-ME,* **59:** 163-167.

Reed-Hill, R.E. (1974) Phsical Metallurgy Principles, Affiliated East-West Press Pvt. Ltd., New Delhi, 709.

Ruud, C.O., Panbgorn, R.N., Dimascio, P.S., Suoha, D.J. (1985) X-ray diffraction measurement of residual stresses in thick, multi-pass steel weldment, *Journal of Pressure Vessel Technology,* **107:** 185-191.

Singh, S.S. (1982) Studies in Mn-Cr-Cu wear resistant white cast Iron, Ph.D. Thesis Department of Metallurgical Engineering, University of Roorkee, India, 155-160.

Verhovene, J.D. (1975) Fundamental of Physical Mettalurgy, John Wiley and Sons, London.

(Received 19/10/1988;
in revised form 07/01/1989)

الاجهادات السطحية المتخلفة في لحام الصلب الكاربوني المعمول تحت الماء

سلمان داود مهدى و سلطان عبدالرزاق سلطان و عبدالكريم فليح حسن

قسم الهندسة الميكانيكية ـ كلية الهندسة ـ جامعة البصرة ـ البصرة ـ العراق

يتضمن البحث إيجاد الاجهادات المتخلفة في سطح اللحام المعمول تحت الماء المالح وذلك باستعمال طريقة حيود الأشعة السينية.

تم ترسيب حزم من اللحام على الواح الصلب الكاربوني وعلى عمق ٢٠٠ ملم تحت سطح كل من الماء المالح (ماء البحر) بتركيز ملوحة مقدارها ٤٠ غم/ لتر والماء العذب (ماء النهر) وذلك باستخدام اسلاك اللحام المعزولة من نوع (Rutile E 7012) وبطريقة لحام نصف آلية. كما تم ترسيب حزم من اللحام على ألواح من نفس الصلب الكاربوني في الهواء لغرض المقارنة.

يشمل البحث مقارنة لنتائج كل من لحام تحت الماء المالح ولحام تحت الماء العذب ولحام الهواء المعمولة جميعاً بنفس تفاصيل ومواصفات اللحام المحددة بثبوت التيار الكهربائي والجهد الكهربائي وسرعة اللحام بالإضافة إلى استعمال نفس النوعية والأقطار لأسلاك اللحام. كما وتم مقارنة هذه النتائج مع نتائج لبحوث أخرى سابقة بنفس الموضوع وكانت نتيجة المقارنة بأن هناك توافقاً نسبياً فيما بينها.

ومن خلال المقارنة وجد أن القيمة العليا لمجموع الاجهادات السطحية المتخلفة في كل من لحام تحت الماء المالح ولحام تحت الماء العذب تعادل ٧٧٪ و ٨١٪ من القيمة العليا لمجموع الاجهادات السطحية المتخلفة في لحام الهواء، على التوالي. كما وجد أن قيمة هذه الاجهادات السطحية المتخلفة في لحام الماء المالح تنقص بمقدار ٥٪ عما هي عليه في لحام تحت الماء العذب. وأظهرت هذه الدراسة ان المقادير العظمى لهذه الاجهادات المتخلفة في لحام تحت الماء المالح وفي

لحام تحت الماء العذب تنحصر ببقعة أقل عرضاً بنسبة ٢٦,٥٪ و٢٢,٧٪ مما هي عليه في لحام الهواء. وأخيراً تستنتج الدراسة ان هذه التغيرات في لحام تحت الماء المالح وفي لحام تحت الماء العذب المتمثلة في اختلاف القيم العليا لمجموع الاجهادات السطحية المتخلفة والمسافات التي تنحصر بها تعود إلى سبب ظروف معدلات التبريد العالية التي تحيط عملية اللحام عند مقارنتها بظروف معدلات التبريد المحيطة بعمليات اللحام في الهواء.